Journal of Archaeological Science 117 (2020) 105136

Contents lists available at ScienceDirect

Journal of Archaeological Science

journal homepage: http://www.elsevier.com/locate/jas

A multi-proxy inference of Jōmon population dynamics using bayesian phase models, residential data, and summed probability distribution of ^{14}C dates

Enrico R. Crema [a,*], Ken'ichi Kobayashi [b]

[a] University of Cambridge, UK
[b] Chūō University, Japan

ARTICLE INFO

Keywords:
Bayesian chronological modelling
Monte-carlo simulation
Jōmon chronology
Prehistoric demography

ABSTRACT

We introduce a new workflow for analysing archaeological frequency data associated with relative rather than absolute chronological time-stamps. Our approach takes into account multiple sources of uncertainty by combining Bayesian chronological models and Monte-Carlo simulation to sample possible calendar dates for each archaeological entity. We argue that when applied to settlement data, this combination of methods can bring new life to demographic proxies that are currently under-used due to their lack of chronological accuracy and precision, and provide grounds for further exploring the limits and the potential of the so-called "dates as data" approach based on the temporal frequency of radiocarbon dates. Here we employ this new workflow by re-examining a legacy dataset that has been used to describe a major population rise-and-fall that occurred in central Japan during the Jōmon period (16,000–2,800 cal BP), focusing on the temporal window between 8,000 and 3,000 cal BP. To achieve this goal we: 1) construct the first Bayesian model of forty-two Jōmon ceramic typology based cultural phases using a sample of 2,120 radiocarbon dates; 2) apply the proposed workflow on a dataset of 9,612 Jōmon pit-dwellings; and 3) compare the output to a Summed Probability Distribution (SPD) of 1,550 radiocarbon dates from the same region. Our results provide new estimates on the timing of major demographic fluctuations during the Jōmon period and reveal a generally good correlation between the two proxies, although with some notable discrepancies potentially related to changes in settlement pattern.

1. Introduction

The last decade witnessed an increasing number of synthetic research studies (Kintigh et al., 2014) where legacy archaeological data, originally collected for different purposes, have been brought together for new purposes. Given the finite nature of the archaeological record (Surovell et al., 2017), it is our collective responsibility to identify opportunities for data reuse, as well as tackle the new types of methodological and theoretical hurdles prompted by this task (Bevan, 2015; Huggett, 2020). Perhaps one of the best examples of such new challenges is the reuse of large collections of radiocarbon dates as a proxy of prehistoric demographic changes. This approach, often referred to as *dates as data* (Rick, 1987), has grown rapidly in its number of applications during the last decade (e.g. Shennan et al., 2013; Crema et al., 2016; Zahid et al., 2016; Bevan et al., 2017; Riris, 2018 etc.), thanks to the increased availability and accessibility of radiocarbon databases (e.g. Chaput and Gajewski, 2016; Manning et al., 2016; Lucarini et al., 2020) and the parallel development of a suite of new statistical techniques designed to handle such data (Brown, 2017; Crema et al., 2016; Crema et al., 2017; Bronk Ramsey, 2017; Timpson et al., 2014; McLaughlin, 2018, etc.).

The *dates as data* approach is, however, not immune to criticisms. Its core assumption (more people → more dateable samples → more radiocarbon dates) has been critically discussed since its inception (see Fig. 1 in Rick, 1987), and several issues have been put forward in the last decade, from the false signals linked to sampling error and the calibration process to deeper concerns on the very nature of the proxy itself (e.g. Attenbrow and Hiscock, 2015, Contreras and Meadows, 2014; Freeman et al., 2018; Torfing, 2015; Williams, 2012; Weninger et al., 2015). While methodological advances have solved many of these challenges, some remain sceptical of the usefulness of the whole enterprise. There is, however, a consensus amongst practitioners (and critics),

* Corresponding author.
E-mail address: erc62@cam.ac.uk (E.R. Crema).

https://doi.org/10.1016/j.jas.2020.105136
Received 8 January 2020; Received in revised form 23 March 2020; Accepted 24 March 2020
Available online 15 April 2020

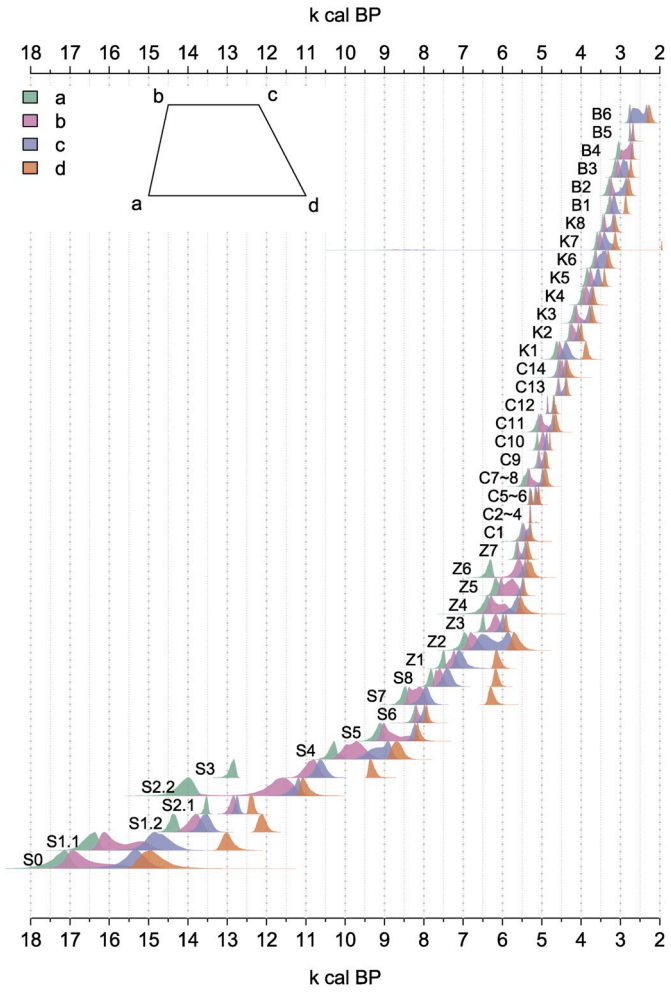

Fig. 1. Marginal posterior distribution of the trapezoidal model parameters for the 42 Jōmon ceramic phases.

that prehistoric population reconstructions should be based on multiple proxies rather than be exclusively reliant on the density of radiocarbon dates. Nonetheless, examples are limited (but see Crombé and Robinson, 2014; Downey et al., 2014; Palmisano et al., 2017; Tallavaara and Pesonen, 2018; Feeser et al., 2019), as most alternative proxies in prehistoric contexts do not offer comparable chronological precision and accuracy to radiocarbon dates. As a consequence, more traditional and perhaps more direct lines of evidence such as site and dwelling counts have been underused due to their temporal definition being based on attributions to cultural phases rather than absolute dates (but see Oh et al., 2017).

1.1. Uncertainties in archaeological periodisations

In order to be able to use proxies that are exclusively defined by chrono-typological phases, we need to be able to assign to each calendar date t a probability of occurrence $P(t)$ of an archaeological event. The objective is thus fundamentally equivalent to the calibration of radiocarbon dates; both measure some physical properties (amount of 14C isotope vs diagnostic traits on artefacts) linked to the flow of time through some process (radiocarbon decay vs cultural transmission) and make use of a statistical model that combines different sources of uncertainty to yield a probabilistic estimate of when a particularly event has occurred (e.g. making a ceramic vessel). In the case of radiocarbon calibration, these are measurement errors in the sample and the uncertainties associated with the calibration curve. In the case of archaeological periodisation, we need to take into account three interrelated forms of uncertainty.

The first one, which we will refer here to as *within-phase uncertainty*, is how we define the shape of the probability density function within the archaeological period assigned to a particular event. In other words, how we describe the change of $P(t)$ when t is within a particular phase? For example, if an event is assigned to a phase dated between 700 and 300 BCE, what is the probability that the event occurred in the year 354 BCE? While ultimately the selection of the most appropriate probability density function is context-dependent, there have been some discussions on what shape we should assume a priori. Proponents of aoristic analysis (e.g. Johnson, 2004; Crema, 2012; Orton et al., 2017) suggest a uniform distribution, and hence would assign a constant probability within the archaeological phase (thus for the example above, $P(t = 354\ \text{BCE})$ would be equal to 0.0025, or 1/400). Crema (2012) justifies this shape invoking the principle of insufficient reason: in the lack of any additional knowledge, we should assume that all years have equal probabilities. This assumption may be valid in crime science (where the aoristic analysis was originally developed, see Ratcliffe and McCullagh, 1998), and perhaps in some historical contexts where an ensemble of chrono-typological, dendrochronological, numismatic, and historical dates are available. However, for prehistoric chrono-typological phases, there is a reasonably large number of theoretical and empirical studies (e.g. Rogers, 1962; Christenson, 1994; Neiman, 1995; Lyman and Harpole, 2002, Manning et al., 2014, Kandler and Crema, 2019, etc.) that suggest a unimodal curve of a rise and fall in popularity (referred to as popularity principle; see O'Brien and Lyman, 2000) to be more appropriate. The literature on chronological apportioning, which deals with similar problems, has indeed adopted such assumption by using probability distributions such as the Chi-square (Carlson, 1983), the Gamma (Steponaitis and Kintigh, 1993), the Beta (Baxter and Cool, 2016), and the normal distributions (both in its truncated or non-truncated forms; Carlson, 1983; Bellanger and Husi, 2012; Roberts et al., 2012; Baxter and Cool, 2016). These alternatives reflect both the general agreement on the unimodal shape and the more context-specific debate on whether the rise and fall in popularity should be assumed to be symmetric or not, or whether there should be flexibility in capturing variation in the kurtosis.

The second form of uncertainty is determined by how we define the membership of a particular archaeological event to a given archaeological phase or period. This type of uncertainty (see Bevan et al., 2012; Crema, 2015 for review), which will refer here to as *phase assignment uncertainty*, is conditioned by the nature of the diagnostic elements used by archaeologists to associate a particular artefact to an archaeological phase. An event can thus be assigned to one or more phases or subphases, with potentially high levels of non-random inter-observer errors (see Bevan et al., 2012 for an example involving potsherd recovered in survey contexts). *Phase assignment uncertainty* is effectively linked with *within-phase uncertainty*, as one could argue that $P(t)$ could be described by a mixture model with k probability density functions, each with a mixture weight which are probabilities that sum to unity. The parameter k will thus represent the range of possible chrono-typological phases, and the weights would represent our degree of belief of a focal event being assigned to each. Estimates of the mixture weights could potentially be derived from properties of the diagnostic elements (see for example Bevan et al., 2012), but in the majority of cases these are unlikely to be reported (i.e. most archaeologists will report "phase A ~ phase B", rather than "70% phase A and 30% phase B"). It is an open question on whether in the absence of precise mixture weights one should assume them to be uniformly distributed, proportional to the duration of each phase (e.g. if phase B has three times the duration of phase A, w_A should be equal to 0.25 and w_B equal to 0.75), or based on observed frequencies of artefacts assigned to each phase (cf Ortman, 2014).

The third form of uncertainty is determined by how the phases themselves are dated. Can we be confident that the phase to which we assigned our event is precisely dated between 700 and 300 BCE, rather

than 711 and 298 BCE? In essence, such *phase boundary uncertainty* is associated with our uncertainty in defining the parameters of the probability density function describing each phase. Nearly three decades of Bayesian chronological models of radiocarbon dates (Buck et al., 1992; Ziedler et al., 1998; Bronk Ramsey, 2009a) have dealt with this problem, enabling archaeologists to infer parameters for a variety of distributions (including flexible options such as the trapezoidal distribution, Lee and Bronk Ramsey, 2012), as well as to incorporate various assumptions in the form of priors and constraints.

Thus, there is a substantial body of archaeological work that tackles these three forms of uncertainties, but little to no attempt has been made to take them into account at the same time. We argue that such partial treatment can lead to substantial biases when examining frequency data. For example, handling *within-phase uncertainty* but ignoring *phase boundary uncertainty* might potentially lead to the false impression that significant changes in temporal frequencies occur at precise intervals corresponding to boundaries between archaeological phases.[1]

The solution proposed in this paper expands the Monte-Carlo approach developed initially in Crema (2012) by utilising Bayesian posterior samples of phase parameters. This effectively involves simulating n possible dates of archaeological events by iteratively: 1) sampling a random start and end date of the assigned phase(s) (*phase boundary uncertainty*); 2) randomly assign the even to a unique phase (*phase assignment uncertainty*); and 3) randomly sample a possible date within such phase (*within-phase uncertainty*). In order to enable full reproducibility (Marwick, 2017), details of this procedure, as well as the R and OxCal scripts utilised for the case study, are available on the following GitHub repository: https://github.com/ercrema/jomonPhasesAndPopulation as well as on zenodo: https://doi.org/10.5281/zenodo.3719507.

1.2. Case study: Jōmon chronology and demography

The Jōmon culture (16,000–2,800 cal BP; Habu, 2004) offers one of the best researched prehistoric hunter-gatherer traditions known to archaeology, thanks to the exceptionally high volume of rescue archaeology in Japan (Habu and Okamura, 2017) combined with the rare opportunity to rely on a ceramic-based chrono-typological sequence. The latter in particular has been central to Japanese archaeology, and nearly a century of painstaking research has led to the creation of detailed regional and sub-regional sequences. As a result, archaeologists utilise more often such relative sequences, rather than absolute calendar dates, when referring to key episodes and events within the Jōmon period.

Given its time span of over 10,000 years, it is perhaps unsurprising that the Jōmon period was characterised by multiple episodes of population booms and busts, typically inferred from fluctuations in the number of residential units (pit-dwellings) and archaeological sites. Early works (Koyama, 1978) have initially identified major regional trends (a slow rise in the Southwest, a rise and fall in the centre, and rise followed by a plateau in the North) at a millennial-scale. However, subsequent studies based on chrono-typological sequences (e.g. Imamura, 1997; Shitara, 2004; Sekine, 2014, etc.) have revealed a much more complex picture, with multiple fluctuations and further regional and sub-regional variation in the demographic trajectories. These studies provide a much-refined perspective on Jōmon demography, potentially capturing key processes such as population dispersal and differences in local adaptive strategies to environmental change. However, the over-reliance on ceramic-based chronology severely limits the possibility to explore these hypotheses by, for example, comparing these dynamics to climatic data, or to infer key measures such as population growth rate accurately. The *dates as data* provide one way to overcome these issues (see Crema et al., 2016 for an application on Jōmon data) but should ideally be coupled with alternative proxies to evaluate its robustness as a measure of past demographic change.

Assigning absolute calendar dates to the Jōmon chrono-typological sequence is thus an important step for further exploring its population dynamics, and at the same bring in additional lines of evidence to test specific hypothesis linked to social, economic, and cultural factors. This objective becomes even more appealing if we consider that the total number of chrono-typological phases and subphases across the entire length of the Jōmon period is easily above 100 (cf. Kobayashi, 2008). This fine-grained scheme had led some scholars to suggest that the duration of several phases might be less than 100 years (e.g. Kobayashi, 2008), an unmatched resolution for prehistoric hunter-gatherers. However, attempts to construct an absolute chronological framework for these ceramic phases have been comparatively limited. Most studies have focused on the visual display of calibrated radiocarbon dates associated with key ceramic phases, which has already revealed putative relationships between major cultural and climatic events throughout the Jōmon period (e.g. Kudo, 2007).

More recently, Kobayashi (2008, 2017) has collated and analysed a sample of over 3,200 radiocarbon dates to develop an absolute chronology of the start and end dates of major Jōmon ceramic phases. Kobayashi's chrono-typological sequence has subsequently been used to construct time-series of residential units counts for different regions (Kobayashi, 2008, Crema, 2012; Crema, 2013), confirming the existence and assessing the timing of at least three cycles of population rise and fall between the Early and the Late Jōmon periods (ca 7000- 3200 cal BP) in central Japan.

However, Kobayashi's sequence assumes perfectly abutting phases (i.e. the start of a ceramic phase coincides to the end of the previous phase), no uncertainty in the dates, and an agnostic view on the *within-phase uncertainty*. As a consequence, some analyses showed a false impression of high accuracy and precision when abrupt changes in the number of residential units were recorded between chronologically adjacent phases. To overcome this issue, here we model Jōmon ceramic phases allowing for overlaps and model the *within-phase uncertainty* using the trapezoidal distribution. The latter allows to take into the assumption of a rise and fall pattern in the popularity of cultural traits while allowing for the flexibility to take different shapes (see Lee and Bronk-Ramsey, 2012). We employ Bayesian inference to fully take into account the uncertainty in the estimates of model parameters and use a nested form of Monte-Carlo simulation to sample absolute calendar dates of archaeological events while taking into account all three forms of uncertainty described above.

Our case study re-examines a dataset of Jōmon pit-dwellings from southwest Kanto (Saitama, Tokyo, and Kanagawa prefectures) and Chubu Highlands (Nagano and Yamanashi prefectures) in central Japan as a case study. The dataset has been originally studied by Imamura (1997) and re-examined by Crema (2012). We then compare the time-series of residential frequencies we obtained from the two regions to the summed probability distribution (SPD) of radiocarbon dates from the same area, examining, in particular, the timing of the Middle Jōmon rise-and-fall, the largest demographic fluctuation recorded in this area during the Jōmon period. Given the smaller number sample size for earlier periods we focus on the interval between 8,000 and 3,000 cal BP, corresponding approximately to the latter half of the Initial Jōmon to the end of the Final Jōmon period.

2. Materials

We collated radiocarbon dates with known association to Jōmon ceramic phases by augmenting an existing database created by one of us

[1] It is also worth noting here that while the formal definitions of these different forms of chronological uncertainties are pivotal in designing the solution detailed below, we are not implying here an essentialist approach towards typological phases, but rather acknowledge them as useful abstractions that capture observed continuous variations of diagnostic elements and their relation to the flow of time.

(see Kobayashi, 2017). The initial dataset has been cleaned by removing duplicates, samples with incomplete information, as well as dates from specimens with suspected marine reservoir effect. The resulting, final dataset consisted of 2,120 radiocarbon dates from 447 archaeological sites across Japan (see electronic Supplementary Table 1). We used a revised form of Kobayashi's ceramic phases (Table 1; see also Kobayashi, 2017) by aggregating shorter and small-sampled sub-phases together. The resulting sequence comprised 42 ceramic phases covering the entire chronological span of the six major Jōmon periods (Initial, Incipient, Early, Middle, Late, and Final Jōmon). Samples of soot and organic residues taken from the same vessel were combined using OxCal's *R_Combine* function under the assumption that the dates were associated with the same calendar year.

The residential data used by Imamura (1997) and Crema (2012) study was collated by digitising summary tables from Suzuki (2006). This consisted of dwelling counts organised by ceramic phases with different degrees of uncertainty ranging from associations to a single phase to as many as 14 phases (see Crema, 2012 for an extensive discussion). The 9,612 Jōmon pit-dwellings in the dataset were collated from Yamanashi (n = 501), Tokyo (n = 2,221), Saitama (n = 1,748), Kanagawa (n = 2,724), and Nagano (n = 2,418) prefectures in central Japan. The sample includes few pit-dwellings dated to the Incipient, Initial, and Final Jōmon periods which are outside the temporal window of analyses in the majority of the Monte-Carlo samples of ceramic phase start and end dates. Nonetheless, we decided to keep the entire dataset, as this has no impact in the approach we employed other than the frequency time-series being composed of slightly different sample sizes for each Monte-Carlo iteration.

For the SPD analysis, we collated a total of 2,544 radiocarbon dates from 370 sites located in the same regions have been retrieved from the National Museum of Japanese History's radiocarbon database (Kudo, 2017, URL: https://www.rekihaku.ac.jp/up-cgi/login.pl?p=param/esrd/db_param, electronic Supplementary Table 2). The initial data obtained from the online query included all dates associated with terrestrial and marine samples attributed to the Jōmon period from the five prefectures. We excluded, from this initial set, duplicates, dates from bones with unknown impact of reservoir effect (n = 13), as well as samples with a ^{14}C age outside the bracket 7,500–2,500 ^{14}C Age (ca. 8000–3000 cal BP). The final dataset consisted of 1,550 radiocarbon dates from 283 sites, with 77 dates also included in the samples used for the Bayesian chronological modelling.

3. Methods

3.1. Bayesian chronological modelling

We fitted trapezoidal models (Lee and Bronk Ramsey, 2012) to the 42 Jōmon ceramic phases using *OxCal* v.4.3 (Bronk Ramsey, 2009a) and bespoke R scripts to handle input/output via the *oxcAAR* v1.0 R package (Hinz et al., 2018). The choice of the trapezoidal model over other distributions was dictated by its flexibility in capturing a variety of possible shapes to portray within-phase uncertainty, including uniform distribution and single-peaked symmetric distributions comparable to the Gaussian. In order to evaluate the sensitivity of our outcome to the choice of this model we also fitted Gaussian and Uniform models which produced results that were qualitatively comparable to the ones presented in the paper (see electronic Supplementary Figs. 1–4).

Radiocarbon dates associated with the same event (e.g. the same ceramic vessel) were combined using the *R_Combine* function in *OxCal* after removing potential outliers (Bronk Ramsey, 2009b) using a normal distribution model with a mean of zero and a standard deviation of 2. This was achieved by removing the date with the highest outlier probability and by repeating the process iteratively until the overall agreement index was above 60 and the Chi-squared test was non-significant at $\square = 0.05$.

The initial fitting of the trapezoidal model for the 42 ceramic phases

Table 1
Correspondence between different nomenclature of ceramic phases and associated sample size of radiocarbon dates (*n* = number of radiocarbon dates, *n(eff.)* = number of radiocarbon dates associated to different specimens; and *Sites* = number of archaeological sites from which samples were recovered). * *Kasori E* ceramic phases have two distinct classifications using Arabic and Roman numerals (see detailed review in Toda, 1999).

Ceramic Phases	n	n (eff.)	Sites	Kobayashi (2017)	Ceramic Phase in Suzuki's Pithouse Data
S0	16	16	4	S0	Mumon doki
S1.1	64	62	16	S1-1	Ryūkisenmon-kei
S1.2	77	77	24	S1-2	Biryūkisenmon-kei; Tsumegatamon-kei
S2.1	94	90	20	S2-1	Tsumegatamon-kei; Ōnatsumon-kei
S2.2	38	38	8	S2-2	Tajōmon-kei
S3	107	107	47	S3-1	Igusa I; Igusa II; Daimaru;
				S3-2	Natsushima; Inaridai;
				S3-3	Tateno; Inarihara;
				S3-4	Ōurayama; Hanawadai 1; Hanawadai 2; Hirasaka;
S4	45	45	24	S4	Mito; Lower Tado; Upper Tado; Hosokubo
S5	22	22	10	S5	Shiboguchi; Nojima
S6	14	14	6	S6	Ugajimadai
S7	48	47	14	S7	Lower Kayama; Upper Kayama
S8	85	80	21	S8	Uenoyama; Irumi I; Irumi II; Ishiyama; Okkōshi; Tenjinyama; Kaminokidai; Shioya; Shimoyoshii
Z1	56	50	16	Z1	Lower Hanazumi
Z2	31	29	15	Z2	Sekiyama; Futatsuki; Kaminoki
Z3	55	53	8	Z3	Kurohama; Ario
Z4	16	14	10	Z4	Moroiso a; Minamiōhara
Z5	59	55	15	Z5	Moroiso b; Uehara
Z6	33	30	15	Z6	Moroiso c; Hinata I; Kagobatake I; Shitajima
Z7	29	29	16	Z7	Jūsanbodai; Hinata II; Kagohata II
C1	10	10	6	C1	Goryōgadai 1
C2~4	19	19	14	C2~C4	Goryōgadai 2
C5~6	22	22	13	C5	Atamadai 1a; Atamadai 1 b;
				C6	Mujinasawa; Katsuzaka I; Aramichi
C7~8	33	32	16	C7	Atamadai 2; Atamadai 3;
				C8	Katsuzaka 2; Tōnai I; Tōnai II;
C9	61	61	28	C9a	Idojiri I;Idojiri III; Katsuzaka
				C9bc	3; Atamadai 4
C10	58	58	23	C10a	Daigi 8a; Kasori E1 (EI)* Sori
				C10b	I
				C10c	
C11	41	41	21	C11ab	Daigi 8 b; Kasori E2 (EI)*;
				C11c	Sori II; Sori III
C12	106	105	30	C12a	Daigi 9; Kasori E3 (EII-EIII)*;
				C12b	Sori IV;SoriV
				C12c	
C13	64	63	23	C13	Kasori E4 (EIV)*; Daigi 10;
C14	11	11	7	–	Kasori EV; Daigi 10;
K1	37	37	23	K1-1	Shōmyōji 1;Shōmyōji 2
				K1-2	
				K1-3	
K2	103	65	17	K2	Horinouchi 1
K3	54	49	16	K3	Horinouchi 2
K4	28	25	11	K4	Kasori B1
K5	58	48	9	K5	Kasori B2
K6	26	24	6	K6	Kasori B3
K7	47	43	16	K7	Takaihigashi; Sōya
K8	39	38	11	K8	Angyō 1; Angyō 2
B1	89	83	29	B1	Ōbora B; Angyō 3a
B2	73	58	25	B2	Ōbora BC; Angyō 3 b
B3	44	41	20	B3	Ōbora C1; Angyō 3c; Maeura 1
B4	54	51	17	B4	Ōbora C2; Angyō 3 d; Maeura 2

(*continued on next page*)

Table 1 (*continued*)

Ceramic Phases	n	n (eff.)	Sites	Kobayashi (2017)	Ceramic Phase in Suzuki's Pithouse Data
B5	58	54	27	B5	Ōbora A; Chiami; Kōri I
B6	96	52	21	B6	Ōbora A'; Arami; Kōri II

returned an overall agreement index of 48. We thus removed a total of 46 dates with agreement indices below 60 and refitted our model achieving an overall agreement index of 110.86. We then used the *MCMC_Sample* function in OxCal and extracted 5,000 posterior samples of the four trapezoidal distribution parameters for each of the 42 ceramic phases.

3.2. Monte-Carlo simulation

We simulated calendar dates for each pit-dwelling in three steps:

1. Sample the four parameters of the trapezoidal model from the joint posterior distribution of each of the 42 ceramic phases.
2. Randomly assign a unique phase to all pit-dwellings associated with multiple candidate phases. The probability of a candidate phase being selected was proportional to its standard deviation, calculated using the equation provided by Dorp and Kotz (2003) for trapezoid distributions. For example, if a residential unit was assigned to phases *I*, *II*, and *III*, with standard deviations 20, 30, and 50, the probability of the assigned phase being *I* is equal to 0.2 (i.e. 20/(20 + 30+50)).
3. Randomly draw a calendar date from the trapezoidal distributions defined in step 1 and associated with a given residential unit in step 2.

This routine — which effectively takes into account within-phase, phase assignment, and phase boundary uncertainties — was repeated 5,000 times. For each repetition set we also: a) computed a univariate kernel density estimate of the simulated dates; and b) grouped and counted residential units falling within 100-years sized temporal blocks between 8,000 and 3,000 cal BP (i.e. 8,000–7,901 cal BP; 7,900–7,801 cal BP; etc.).

3.3. Summed probability distribution of radiocarbon dates

A Summed Probability Distribution of Radiocarbon Dates (SPD) was created using the *rcarbon* v.1.3 package (Bevan and Crema, 2019). We calibrated the ^{14}C dates using the *IntCal13* calibration curve (Reimer et al., 2013) and without normalisation to avoid artificial peaks (cf. Weninger et al., 2015). Marine dates were calibrated with the *Marine13* calibration curve (Reimer et al., 2013), using a ΔR of 88 and an associated error of 33 years (Shishikura et al., 2007). To account for inter-site variation in sampling intensity, we summed to unity dates from the same site with a median calibrated age inter-distance of 200 years (cf. Timpson et al., 2014, see electronic Supplementary Fig. 5 for sensitivity analysis with different inter-distance settings). The resulting 768 "bins" have been combined to produce the final SPD curve. To facilitate the comparison between different proxies we aggregated the summed probabilities using the same 100-years temporal blocks between 8,000 and 3,000 cal BP used for the pit-dwelling data. We also sampled random calendar dates from each of the 768 bins and generated time-series of bin counts aggregated using the same 100-years temporal blocks. This process was repeated 5,000 times in order to produce the same number of frequency time-series as the residential units.

3.4. Correlation analysis and model testing

We assessed the correlation between the two demographic proxies by computing 5,000 Pearson's correlation coefficients between randomly paired100-years block time-series of radiocarbon bins and pit-dwelling counts. To explore possible temporal variations in the extent of correlation between the two proxies we also calculated their rolling correlation using a moving window of 10 time-blocks, equivalent to a 1,000 years.

In order to further explore differences between the two demographic proxies, while taking into account the idiosyncrasies of the calibration process and the effects of sampling error, we also employed a modified version of the Monte Carlo testing approach used in Shennan et al. (2013, see also Timpson et al., 2014). The original approach consists of 1) fitting a theoretical growth model to the observed data; 2) simulating the same number of dates as the observed data in calendar time using the fitted model; 3) back-calibrating each date in ^{14}C age and calibrating it back in calendar time; 4) generating a realisation of the theoretical SPD by summing the dates; and 5) repeating steps 1 to 4 multiple times to generate a simulation envelope to which the observed SPD can be compared to. We made two notable changes to this procedure. First, we generated our simulation envelope (representing our theoretical expectation) from the mean value in the composite kernel density estimate of the residential data rather than a fitted exponential curve. Thus, our null hypothesis was that changes in the density of radiocarbon dates are comparable to changes in the density of residential units. Second, we compared observed and simulated annual growth rates rather than the raw SPDs to avoid the impact of early divergences in defining later differences between the two proxies.

4. Results

Fig. 1 shows the posterior distribution of the trapezoidal model parameters of the forty-two Jōmon ceramic phases we examined. Although the Bayesian model did not include any constraints on the temporal relationship between phases, our results confirmed the general sequence expected from the literature, particularly when the "core stage" of each phase (i.e. the interval between the parameters *b* and *c*) was considered. In very few cases the early tail of the distribution (i.e. parameter *a*) exhibited reverse chronological order (e.g. $S2.1_a$ is estimated to be more recent than $S2.2_a$; $S6_a$ is more recent than $S7_a$), but these exceptions were limited to chrono-typological phases of the Initial Jōmon period where the number of diagnostic elements in the ceramics are limited.

The increase in the number of more complex decorative elements does undoubtedly play a significant role in explaining the more detailed periodisation and consequently the shorter duration of ceramic phases in some temporal windows, most notably within the Middle Jōmon period. These shorter phases (some possibly with sub-century durations) often have a higher degree of overlap in their interval. In the case of the Middle Jōmon period, this pattern can at least in part be explained by the presence of plateaus in the calibration curve (particularly around 5,300 to 5,000 cal BP). More in general, and aside from the genuine existence of overlaps between phases, it is worth considering that the model does not take into account the spatial dimension, and consequently the diffusion of particular ceramic styles and the resulting temporal discrepancy across sites located in different regions. These are, however, acceptable limitations as the pit-dwelling data we examined are from central Japan which has the most substantial contribution to the data we used to define our chronological model. Nonetheless, targeted studies on smaller regions and/or explicit incorporation of the spatial dimension are desirable if more accurate regional comparisons are being sought.

Fig. 2 shows the composite plots of the kernel density estimates (CKDE; Brown, 2017) obtained from each of the 5,000 simulates sets of pit-dwelling dates from Southwest Kanto (Kanagawa, Saitama, and Tokyo prefectures; Fig. 2-a) and Chubu highlands (Yamanashi and Nagano prefectures; Fig. 2-b). Both sets of curves capture the main demographic fluctuations depicted in Imamura's original study (cf. fig. 2 in Imamura, 1997), including the Early Jōmon rise and fall (ca. 6,500–5,800 cal BP) and the minor oscillations between the end of Middle Jōmon

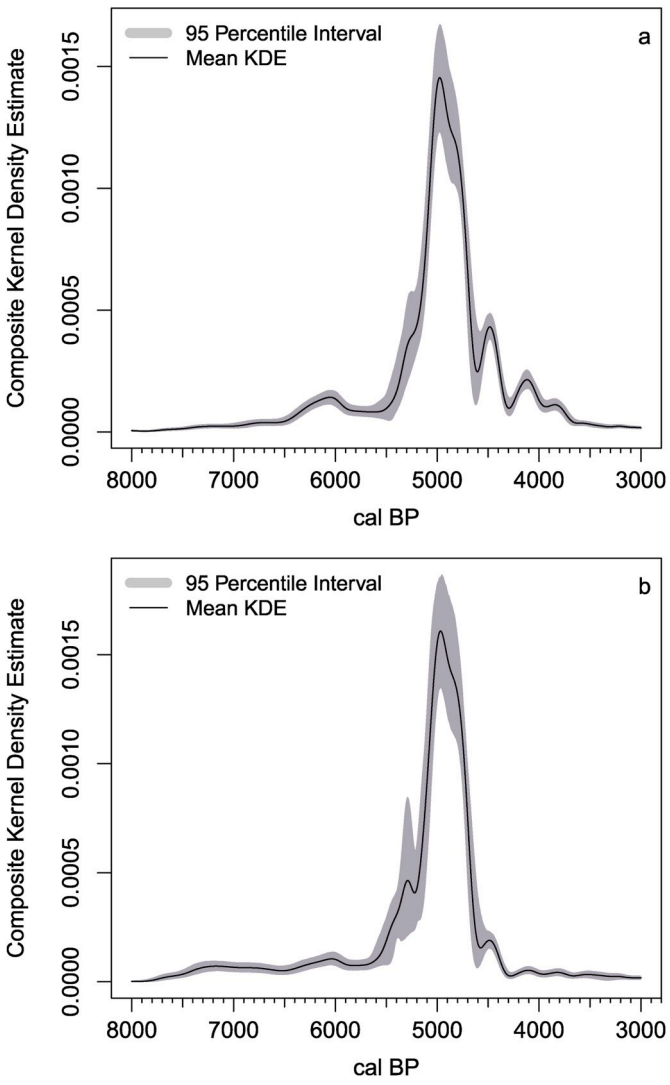

Fig. 2. Composite kernel density estimates derived from the simulated dates of Jōmon pit-dwellings from Southwest Kanto (a) and Chubb highland (b). The envelope represents the 95% percentile interval of the kernel densities across the 5,000 simulations, and the solid line the average value for each calendar date.

and the first half of the Late Jōmon period (ca. 4,600–4,000 cal BP) observed in Southwest Kanto, and most notably the Middle Jōmon boom and bust (ca. 5,500–4,600 cal BP) observed in both regions.

The combined time-series of the two regions (Fig. 3-a) shows broad similarities in shape with the SPD generated from the radiocarbon dates of the five prefectures (Fig. 3-b). The latter also exhibits boom and bust events over the same interval, although with some discrepancies in their timing (see below), the lack of a rise-and-fall pattern in the mid 5th millennium cal BP, and a comparatively higher density of dates from 4,700 cal BP onwards. Despite these differences, the overall sample correlation between the two time-series across the 5,000 Monte-Carlo iterations was high (median: $r = 0.65$; 95% percentile interval: 0.51–0.75) and the 1,000 years rolling correlation (Fig. 3-b) suggest a generally high agreement between the time-series of radiocarbon dates and pit-dwellings.

The discrepancies in the timing of the Middle Jōmon rise and fall between the 6th and the 5th millennium cal BP are further highlighted in Fig. 4, where the observed annual growth rate computed from the radiocarbon dates is compared against a theoretical envelope of growth rates simulated from the observed residential data. The analysis confirms intervals when the SPD-based growth rates diverge significantly from the expectation derived from residential data, with lower rates around 5,500–5,350 and 5,100–4,900 cal BP, and higher rates around 4,800–4,300 and 4,000 cal BP.

5. Discussion

The Bayesian chronological model presented here is most likely the first of many attempts in providing a more accurate chrono-typological sequence for the Jōmon period. We intentionally decided to not present point-estimates of the start/end date of the ceramic phases to avoid conveying a false impression of a precision that cannot be realistically achieved. We argue, instead, that conversions from a relative to an absolute chronological framework should fully embrace all forms of uncertainty, including those defining the chronological boundaries of individual phases and periods.

Our case study demonstrates the importance and implications of defining a statistical framework for chrono-typological phases. This paper constitutes the third attempt, after Imamura (1997) and Crema (2012), in generating a time-series of pit-dwelling frequency based on the same original data. Although both previous works and our analyses have highlighted comparable fluctuations in the number of residential units, there are some notable differences in the timing of these events that are worth noting. Perhaps the most relevant case is the Middle Jōmon rise and fall. Imamura (1997) original work was based on an earlier chronology based on uncalibrated dates, with the rise of the Middle Jōmon "boom" dated at ca. 5,000 bp (ca. 5700 cal BP) and the decline after 4,400 bp (ca 5000 cal BP), while Crema (2012) reassessment suggested the rise starting from 5,500 cal BP and the decline from 4,700 cal BP. Our analysis has instead revealed that the increase in population size started at 5500 cal BP (confirming the results of Crema, 2012) with the decline stage starting as earlier as 4,900 cal BP (thus somewhat closer to Imamura's original estimate). The implication of an earlier onset of the Middle Jōmon decline is particularly noteworthy as it cast further doubts on the established narrative of a mid-5th millennium cooling or the 4.2 k event as a driver of the population decline (c.f. Imamura, 1997; Yasuda, 2004; Suzuki, 2009; Tsuji, 2013; Taniguchi, 2019).

The absolute chronological framework offered by the combination of Bayesian modelling and Monte-Carlo simulation has also enabled an evaluation of the *dates as data* approach, following similar works carried out by few others (e.g. Palmisano et al., 2017, Tallavaara and Pesonen, 2018). Our results indicate an overall agreement across the two proxies, reinforcing the evidence of multiple episodes of possible demographic fluctuations between 8,000 and 3,000 years ago. However, we also identified several notable discrepancies: the SPD curve shows an earlier timing of the Middle Jōmon rise-and-fall and an overall higher relative density of dates during the Late and Final Jōmon (i.e. ca 4,500 to 3,000 cal BP).

One plausible explanation for these discrepancies is the major shift from nucleated to a dispersed settlement pattern between the Middle and the Late Jōmon periods (Taniguchi, 2005, Crema, 2013, see Palmisano et al., 2017 for similar interpretations in Central Italy). The binning protocol used in this paper and elsewhere (cf. Timpson et al., 2014) reduces the effect of inter-site variation in sampling intensity, but effectively makes the SPD a proxy of settlement density that disregards size variation. It follows that if the number of settlements is reduced, but the average size increased due to nucleation, the SPD might signal a decline while the time series of residential density show the opposite trend. Similarly, an episode of dispersion and settlement fission to smaller communities might show an increase in the SPD (larger number of sites) matched with a decrease in residential density (smaller number of residential units).

Thus one possible hypothesis that could explain the mismatch observed in Fig. 3 can be summarised as follows: 1) the faster (and earlier) increase in the SPD around 5400 cal BP is the result of an episode of territorial expansion and repeated episodes of settlement fission; 2)

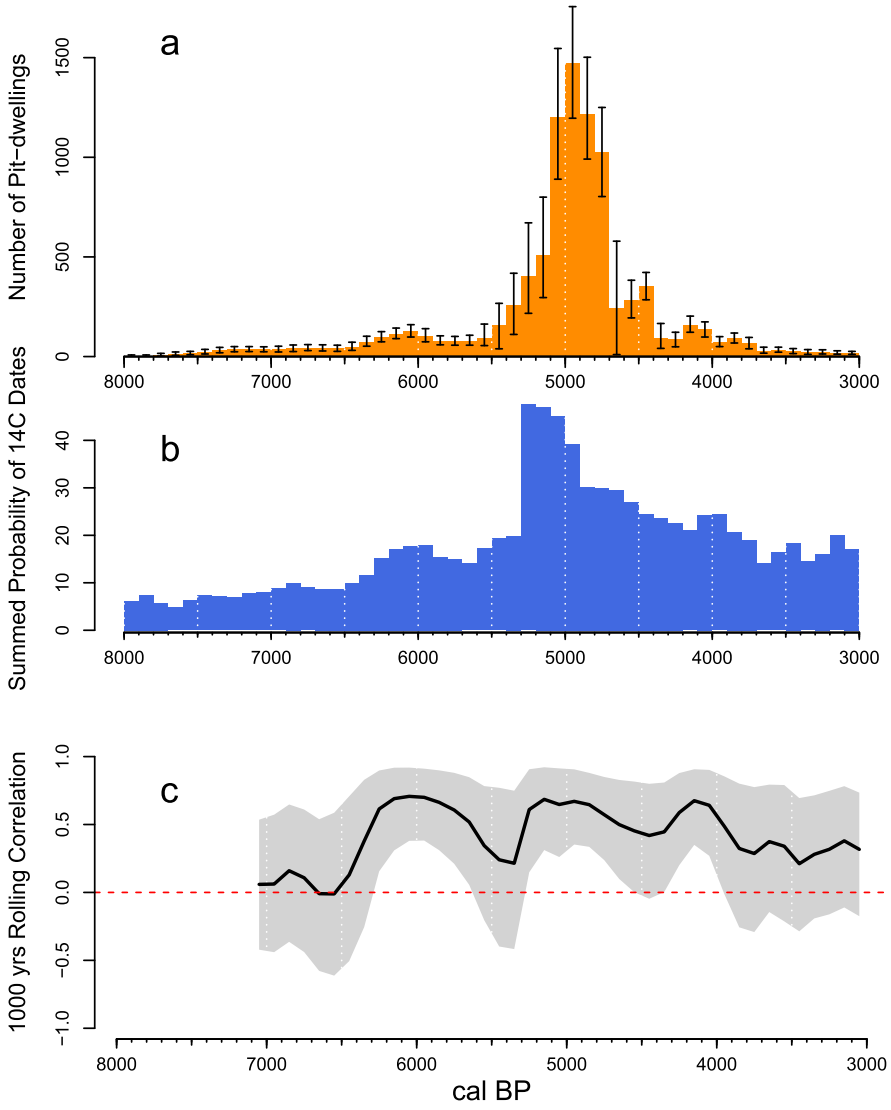

Fig. 3. Temporal frequencies of residential units (a) and summed probability of radiocarbon dates (b) and their correlation over a 1,000 years moving window (c). Error bars in panel a and the grey envelope in panel c are based on 95% percentile interval across the 5,000 Monte Carlo simulations.

the subsequent decline in the SPD during the peak in residential density is the outcome of settlement nucleation and population growth; and 3) the overall higher relative density of SPD during the first few centuries of the 5th millennium is a signature of fission events to smaller settlements. A similar small mismatch between site counts and dwelling counts have been observed elsewhere and has indeed been explained by episodes of nucleation/dispersions (e.g. Crema, 2013, see also below). Unfortunately, the pit-dwelling count data provided by Suzuki does not record membership of individual pit-dwelling to specific settlements, and hence this hypothesis cannot be directly tested in this context by comparing the SPD to a time-series of occupied settlements.

Archaeological evidence does, however, suggest several significant changes in the settlement pattern during the second half of the Middle Jōmon period (phases C11∼C14 here). Stratigraphic evidence shows an overall decrease in the occupational span of individual pit-dwellings between the Kasori E2 (phase C11) and the Kasori E3 (phase C12) phases, with the latter characterised by shorter, repeated re-occupations in large nucleated settlements (Kobayashi, 2016). As a consequence, the same temporal window was characterised by a higher number of residential units that do not necessarily translate into an increase in the underlying population size. During the subsequent Kasori E4 phase (phase C13) these large settlements fissioned into smaller sites, with a much shorter occupational span that suggests an increased level of residential mobility (Kobayashi, 2004). This shift from nucleated to dispersed settlement patterns have been commonly explained as the consequence of a change in subsistence economy triggered by the 4.2 cooling event (c.f. Suzuki, 2009). However, the possibility of local resource overexploitation cannot be dismissed, especially considering how the cooling event has most likely occurred after the shift in settlement pattern and the decline in the number of pit-dwellings (Kobayashi, 2004). An interesting parallel could also be drawn to the growth and decline of major Jōmon settlements such as Sannai-Maruyama in Northern Japan. Habu (2008) hypothesise that a plant-based subsistence intensification (e.g. chestnuts and other nuts) sustained the initial growth of this and possibly other settlements in the region. This increased over-specialisation, however, made Jōmon communities overpopulated and increasingly less resilient to episodes of minor climatic fluctuations affecting plant productivity, eventually leading to the demise of large nucleated settlements. Similar 'rigidity traps' (Carpenter and Brock, 2008) might have occurred in Central Japan as well, but further studies integrating demographic, climatic, and subsistence data will be necessary to explore this hypothesis in detail.

The availability of an absolute chronological framework enables us to make tentative estimates of the annual percentage growth rate

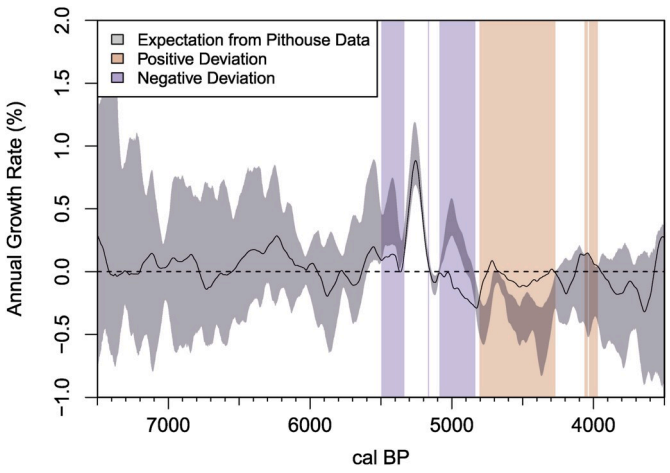

Fig. 4. Statistical comparison of the observed annual growth rate in the SPD (solid line) and the simulated 95% percentile envelope based on the temporal frequencies of residential units obtained from composite kernel density estimate analysis. Regions highlighted in red indicate intervals where the SPD-based growth rate is higher than the residential density based growth rates. Regions highlighted in blue suggest the opposite (i.e. lower growth rates in the SPD). The temporal range of the analysis is reduced by 400 years on both ends to limit edge effects. The global P-value was equal to 0.0009. (For interpretation of the references to colour in this figure legend, the reader is referred to the Web version of this article.)

observed during the Jōmon period. For example, the annual growth rate during the Middle Jōmon "boom" (between 5,500–5,400 and 5,000–4,900 cal BP) was 0.45% (95% percentile interval: 0.33–0.74%) for the pit-dwelling data and 0.09% (95% percentile interval: −0.01–0.21%) for the radiocarbon dates, an order of magnitude above the long-term average recorded for hunter-gathers elsewhere (see Zahid et al., 2016) but within the range expected for shorter-term fluctuations (see also Bettinger, 2016). The discrepancies between the two figures are in part due to the different timing of the events (see Fig. 3), and the fact that the SPD should be interpreted as a proxy of settlement growth rate rather than population growth rate.

While these are promising results, there are several challenges both from the standpoint of paleo-demographic inference and the methods presented here. Aside from shifts in settlement pattern, we also need to consider potential changes in the *duration* of archaeological events. Both intra- and inter-annual variations in the length of site occupation could change the ratio between site counts and population size and hence, for example, potentially lead to false signals in SPD depending on the choice of the bin size for aggregating radiocarbon dates from the same site. The same problem applies to the duration of residential units (see above). Ethnographic accounts and archaeological evidence suggest that pit-dwellings can have different duration, lasting somewhere between 3 and 15 years (Watanabe, 1986; Muto, 1995). Variations in residential stability can thus yield higher or lower number pit-dwellings in a given time-window. In the case of Jōmon period, Kobayashi (1991) has inferred from the number of seasonal rebuildings of hearths a maximum use of 8 years for Initial Jōmon pit-dwellings, while for the late Middle Jōmon period, stratigraphic evidence of overlapping features and ^{14}C dates suggest an average occupation span of ca. 13 years, suggesting temporal variations in the use-life of residential units (Kobayashi, 2004). Habu (2001) has also extensively examined residential data and lithic assemblage of the second half of the Early Jōmon period in the same area, providing evidence for sub-regional variations and temporary shifts between collector and forager-like strategies.

The development of a reliable regional Bayesian chronological model of archaeological phases has also its own challenges. While in stratigraphic contexts many of the assumptions that act as priors and/or constraints in the chronological modelling can be well supported, the same degree of confidence cannot be easily justified when we are considering multiple sites located in a wider geographic area and examined potentially with different sampling strategies. For example, a strongly imbalanced data might "pull" the posterior estimates of a particular ceramic phase towards the occupation period of a particular site that happened to have a larger sample of radiocarbon dates. The use of hierarchical models (cf. Banks et al., 2019), or the formal integration of the spatial dimension are desirable directions to be undertaken in order to solve at least some of these issues.

6. Conclusion

Notwithstanding the challenges entailed by developing Bayesian models of chrono-typological sequences, the ability to use an absolute chronological framework while simultaneously accounting for different forms of uncertainty is a crucial step for reusing legacy data in archaeology. Our case study showcases both the necessity and the potential benefits of such an endeavour, particularly in the context of prehistoric demography where the lack of alternative proxies to radiocarbon dates can severely limit the assessment of the reliability of demographic reconstructions as well as the opportunity to identify and test key covariates and hypotheses.

From the perspective of Jōmon archaeology, the comparison between SPDs and residential data has provided an initial assessment of the temporal scale at which settlement dynamics can no longer be ignored, and the choice of the population proxy becomes relevant. At coarser temporal scales of 500–1000 years the agreement between the two proxies is robust and reassuring, but below these thresholds, we identified some noticeable differences in the timing and the magnitude of specific fluctuations that need to be accounted for. These conclusions are context-specific and while they cannot be easily extrapolated to other regions or periods, offer the foundation for future research in prehistoric demography.

Declaration of competing interests

The authors declare that they have no known competing financial interests or personal relationships that could have appeared to influence the work reported in this paper.

Acknowledgements

This research was funded by the ERC grant Demography, Cultural Change, and the Diffusion of Rice and Millets during the Jōmon-Yayoi transition in prehistoric Japan (ENCOUNTER) (Project N. 801953, PI: Enrico Crema). We would like to thank the two reviewers (David Orton and an anonymous) for their constructive comments that helped improve the original manuscript.

Appendix A. Supplementary data

Supplementary data to this article can be found online at https://doi.org/10.1016/j.jas.2020.105136.

References

Attenbrow, V., Hiscock, P., 2015. Dates and demography: are radiometric dates a robust proxy for long-term prehistoric demographic change? Archaeol. Ocean. 50, 30–36. https://doi.org/10.1002/arco.5052.

Banks, W.E., Bertran, P., Ducasse, S., Klaric, L., Lanos, P., Renard, C., Mesa, M., 2019. An application of hierarchical Bayesian modeling to better constrain the chronologies of Upper Paleolithic archaeological cultures in France between ca. 32,000–21,000 calibrated years before present. Quat. Sci. Rev. 220, 188–214. https://doi.org/10.1016/j.quascirev.2019.07.025.

Baxter, M.J., Cool, H.E.M., 2016. Reinventing the wheel? Modelling temporal uncertainty with applications to brooch distributions in Roman Britain. J. Archaeol. Sci. 66, 120–127. https://doi.org/10.1016/j.jas.2015.12.007.

Bellanger, L., Husi, P., 2012. Statistical tool for dating and interpreting archaeological contexts using pottery. J. Archaeol. Sci. 39, 777–790. https://doi.org/10.1016/j.jas.2011.06.031.
Bettinger, R.L., 2016. Prehistoric hunter–gatherer population growth rates rival those of agriculturalists. Proc. Natl. Acad. Sci. Unit. States Am. 113, 812–814. https://doi.org/10.1073/pnas.1523806113.
Bevan, A., 2015. The data deluge. Antiquity 89, 1473–1484. https://doi.org/10.15184/aqy.2015.102.
Bevan, A., Conolly, J., Hennig, C., Johnston, A., Quercia, A., Spencer, L., Vroom, J., 2012. Measuring chronological uncertainty in intensive survey finds. Archaeometry 55, 318–328.
Bevan, A., Colledge, S., Fuller, D., Fyfe, R., Shennan, S., Stevens, C., 2017. Holocene fluctuations in human population demonstrate repeated links to food production and climate. Proc. Natl. Acad. Sci. Unit. States Am. 114, E10524–E10531. https://doi.org/10.1073/pnas.1709190114.
Bevan, A., Crema, E.R., 2019. Rcarbon v1.3.0: methods for calibrating and analysing radiocarbon dates. https://CRAN.R-project.org/package=rcarbon.
Bronk Ramsey, C., 2009a. Bayesian analysis of radiocarbon dates. Radiocarbon 51, 337–360. https://doi.org/10.1017/S0033822200033865.
Bronk Ramsey, C., 2009b. Dealing with outliers and offsets in radiocarbon dating. Radiocarbon 51, 1023–1045.
Bronk Ramsey, C., 2017. Methods for summarizing radiocarbon datasets. Radiocarbon 59, 1809–1833. https://doi.org/10.1017/RDC.2017.108.
Brown, W.A., 2017. The past and future of growth rate estimation in demographic temporal frequency analysis: biodemographic interpretability and the ascendance of dynamic growth models. J. Archaeol. Sci. 80, 96–108. https://doi.org/10.1016/j.jas.2017.02.003.
Buck, C.E., Litton, C.D., Smith, A.F.M., 1992. Calibration of radiocarbon results pertaining to related archaeological events. J. Archaeol. Sci. 19, 497–512. https://doi.org/10.1016/0305-4403(92)90025-X.
Carlson, D.L., 1983. Computer analysis of dated ceramics: estimating dates and occupational ranges. SE. Archaeol. 2, 8–20.
Carpenter, S., Brock, W., 2008. Adaptive capacity and traps. Ecol. Soc. 13 (no. 2) https://doi.org/10.5751/ES-02716-130240.
Chaput, M.A., Gajewski, K., 2016. Radiocarbon dates as estimates of ancient human population size. Anthropocene, AAG hum-induce envir chg 15, 3–12. https://doi.org/10.1016/j.ancene.2015.10.002.
Christenson, A.L., 1994. A test of mean ceramic dating using well-dated kayenta anasazi sites. KIVA 59, 297–317.
Contreras, D.A., Meadows, J., 2014. Summed radiocarbon calibrations as a population proxy: a critical evaluation using a realistic simulation approach. J. Archaeol. Sci. 52, 591–608. https://doi.org/10.1016/j.jas.2014.05.030.
Crema, E.R., 2012. Modelling temporal uncertainty in archaeological analysis. J. Archaeol. Method Theor 19, 440–461.
Crema, E.R., 2013. Cycles of change in Jōmon settlement: a case study from Eastern Tokyo Bay. Antiquity 87, 1169–1181.
Crema, E.R., 2015. Time and probabilistic reasoning in settlement analysis. In: Barceló, J. A., Bogdanovic, I. (Eds.), Mathematics and Archaeology. CRC Press, Boca Raton, pp. 314–334.
Crema, E.R., Habu, J., Kobayashi, K., Madella, M., 2016. Summed probability distribution of 14 C dates suggests regional divergences in the population dynamics of the Jōmon period in Eastern Japan. PloS One 11, e0154809. https://doi.org/10.1371/journal.pone.0154809.
Crema, E.R., Bevan, A., Shennan, S., 2017. Spatio-temporal approaches to archaeological radiocarbon dates. J. Archaeol. Sci. 87, 1–9. https://doi.org/10.1016/j.jas.2017.09.007.
Crombé, P., Robinson, E., 2014. 14C dates as demographic proxies in Neolithisation models of northwestern Europe: a critical assessment using Belgium and northeast France as a case-study. J. Archaeol. Sci. 52, 558–566. https://doi.org/10.1016/j.jas.2014.02.001.
Dorp, J.R. van, Kotz, S., 2003. Generalized trapezoidal distributions. Metrika 58, 85–97. https://doi.org/10.1007/s001840200230.
Downey, S.S., Bocaege, E., Kerig, T., Edinborough, K., Shennan, S., 2014. The neolithic demographic transition in Europe: correlation with juvenility index supports interpretation of the summed calibrated radiocarbon date probability distribution (SCDPD) as a valid demographic proxy. PloS One 9, e105730. https://doi.org/10.1371/journal.pone.0105730.
Feeser, I., Dörfler, W., Kneisel, J., Hinz, M., Dreibrodt, S., 2019. Human impact and population dynamics in the neolithic and bronze age: multi-proxy evidence from north-western central Europe. Holocene 29, 1596–1606. https://doi.org/10.1177/0959683619857223.
Freeman, J., Byers, D.A., Robinson, E., Kelly, R.L., 2018. Culture process and the interpretation of radiocarbon data. Radiocarbon 60, 453–467. https://doi.org/10.1017/RDC.2017.124.
Habu, J., 2001. Subsistence-Settlement Systems and Intersite Variability in the Moroiso Phase of the Early Jōmon Period of Japan. International Monographs in Prehistory, Ann Arbor.
Habu, J., 2004. Ancient Jōmon of Japan. University of Cambridge Press, Cambridge.
Habu, J., 2008. Growth and decline in complex hunter-gatherer societies: a case study from the Jōmon period Sannai Maruyama site, Japan. Antiquity 82, 571–584.
Habu, J., Okamura, K., 2017. Japanese archaeology today: new developments, structural undermining and prospects for disaster archaeology. In: Habu, J., Olsen, W., L'ape, P.V. (Eds.), Handbook of East and Southeast Asian Archaeology. Springer, New York, pp. 11–25.
Hinz, M., Schmid, C., Knitter, D., Tietze, C., 2018. oxcAAR: interface to 'OxCal' radiocarbon calibration. R package version 1.0.0. https://CRAN.R-project.org/package=oxcAAR.
Huggett, J., 2020. Is big digital data different? Towards a new archaeological paradigm. J. Field Archaeol. 45, S8–S17. https://doi.org/10.1080/00934690.2020.1713281.
Imamura, K., 1997. Jōmon jidai no jūkyoatosū to jinkō no hendō. In: Fujimoto, T. (Ed.), Jū No Kōkogaku. Dōseisha, Tokyo, pp. 45–60 (In Japanese).
Johnson, I., 2004. Aoristic Analysis: seeds of a new approach to mapping archaeological distributions through time. In: Ausserer, K.F., ¨rner, W.B., Goriany, M., ckl, L.K.-V. (Eds.), [Enter the Past] the E-Way into the Four Dimensions of Cultural Heritage: CAA2003. BAR International Series 1227. Archaeopress, Oxford, pp. 448–452.
Kandler, Anna, Crema, Enrico, 2019. Analysing Cultural Frequency Data: Neutral Theory and Beyond. In: Prentiss, Anna Marie (Ed.), Handbook of Evolutionary Research in Archaeology. Springer, pp. 83–108.
Kintigh, K.W., Altschul, J.H., Beaudry, M.C., Drennan, R.D., Kinzig, A.P., Kohler, T.A., Limp, W.F., Maschner, H.D.G., Michener, W.K., Pauketat, T.R., Peregrine, P., Sabloff, J.A., Wilkinson, T.J., Wright, H.T., Zeder, M.A., 2014. Grand challenges for archaeology. Am. Antiq. 79, 5–24. https://doi.org/10.7183/0002-7316.79.1.5.
Kobayashi, K., 1991. Jōmonjidai-sōkikōyō no minami-Kantō ni okeru kyojūkatsudō. Jōmonjidai 2, 81–118 (In Japanese).
Kobayashi, K., 2004. Jōmonshakai-kenkyū No Shinshiten: Tanso 14 Nendaisokutei No Riyō. Tokyo, Rokuichishōbō. (In Japanese).
Kobayashi, K., 2008. Jōmonjidai no rekinendai. In: Kosugi, Y., Taniguchi, Y., Nishida, Y., Mizunoe, W., Yano, K. (Eds.), Rekishi No Monosashi: : Jōmonjidai Kenkyū No Hennentaikei. Douseisha, Tokyo, pp. 257–269 (In Japanese).
Kobayashi, K., 2016. Shūraku no kanjōka-keisei to jikan. In: Kobayashi, K. (Ed.), Kōkogaku No Chihei 1. Rokuichishōbō, Tokyo, pp. 65–93 (In Japanese).
Kobayashi, K., 2017. Jōmonjidai No Jitsunendai. Dōseisha, Tokyo (In Japanese).
Kobayashi, T., 2008. Jōmondoki no yōshiki to keishiki. In: Kobayashi, T. (Ed.), Sōran Jōmondoki. Amu Promotion, Tokyo, pp. 2–12 (In Japanese).
Koyama, S., 1978. Jōmon subsistence and population. Senri Ethnol. Stud. 2, 1–65.
Kudo, Y., 2007. The temporal correspondences between the archaeological chronology and environmental changes from 11,500 to 2,800 cal BP on the Kanto plain, Eastern Japan. Quat. Res. 46, 187–194.
Kudo, Y., 2017. Isekihakkutsuchōsa-hōkokusho hōshasei-tansonendai sokutei database no sakusei no torikumi. Nihondaiyonkigakkai kōen yoshi shū 47, 22 (In Japanese).
Lee, S., Bronk Ramsey, C., 2012. Development and application of the trapezoidal model for archaeological chronologies. Radiocarbon 54, 107–122. https://doi.org/10.2458/azu_js_rc.54.12397.
Lucarini, G., Wilkinson, T., Crema, E.R., Palombini, A., Bevan, A., Broodbank, C., 2020. The MedAfriCarbon radiocarbon database and web application. Archaeological dynamics in mediterranean africa, ca. 9600–700 BC. J. Open Archaeol. Data 8, 1. https://doi.org/10.5334/joad.60.
Lyman, R.L., Harpole, J.L., 2002. A. L. Kroeber and the measurement of time's arrow and time's cycle. J. Anthropol. Res. 58, 313–338.
Marwick, B., 2017. Computational reproducibility in archaeological research: basic principles and a case study of their implementation. J. Archaeol. Method Theor 24, 424–450. https://doi.org/10.1007/s10816-015-9272-9.
Manning, K., Timpson, A., Colledge, S., Crema, E., Edinborough, K., Kerig, T., Shennan, S., 2014. The chronology of culture: a comparative assessment of European Neolithic dating approaches. Antiquity 88, 1065–1080.
Manning, K., Colledge, S., Crema, E., Shennan, S., Timpson, A., 2016. The cultural Evolution of neolithic Europe. EUROEVOL dataset 1: sites, phases and radiocarbon data. J. Open Archaeol. Data 5. https://doi.org/10.5334/joad.40.
McLaughlin, T.R., 2018. On applications of space–time modelling with open-source 14C age calibration. J. Archaeol. Method Theor. https://doi.org/10.1007/s10816-018-9381-3.
Muto, Y., 1995. Minzokushi kara mita Jōmon-jidai no tateana-jūkyo. Teikyo Daigaku Yamanashi bunkazai kenkyūjo kenkyū-hōkoku 6, 267–301 (In Japanese).
Neiman, F.D., 1995. Stylistic variation in evolutionary perspective: inferences from decorative diversity and interassemblage distance in Illinois woodland ceramic assemblages. Am. Antiq. 60, 7–36.
O'Brien, M.J., Lyman, R.L., 2000. Applying Evolutionary Archaeology: A Systematic Approach. Kluwer Academic, New York.
Oh, Y., Conte, M., Kang, S., Kim, J., Hwang, J., 2017. Population fluctuation and the adoption of food production in prehistoric korea: using radiocarbon dates as a proxy for population change. Radiocarbon 59, 1761–1770.
Ortman, S.G., 2014. Uniform probability density analysis and population history in the northern rio grande. J. Archaeol. Method Theor 1–32. https://doi.org/10.1007/s10816-014-9227-6.
Orton, D., Morris, J., Pipe, A., 2017. Catch per unit research effort: sampling intensity, chronological uncertainty, and the onset of marine fish consumption in historic london. Open Quat. 3 https://doi.org/10.5334/oq.29.
Palmisano, A., Bevan, A., Shennan, S., 2017. Comparing archaeological proxies for long-term population patterns: an example from central Italy. J. Archaeol. Sci. 87, 59–72. https://doi.org/10.1016/j.jas.2017.10.001.
Ratcliffe, J.H., McCullagh, M.J., 1998. Aoristic crime analysis. Int. J. Geogr. Inf. Sci. 12, 751–764.
Reimer, P.J., Bard, E., Bayliss, A., Beck, J.W., Blackwell, P.G., Ramsey, C.B., Buck, C.E., Cheng, H., Edwards, R.L., Friedrich, M., Grootes, P.M., Guilderson, T.P., Haflidason, H., Hajdas, I., Hatté, C., Heaton, T.J., Hoffmann, D.L., Hogg, A.G., Hughen, K.A., Kaiser, K.F., Kromer, B., Manning, S.W., Niu, M., Reimer, R.W., Richards, D.A., Scott, E.M., Southon, J.R., Staff, R.A., Turney, C.S.M., Plicht, J.V.D., 2013. IntCal13 and Marine13 radiocarbon age calibration curves 0–50,000 Years cal BP. Radiocarbon 55, 1869–1887. https://doi.org/10.2458/azu_js_rc.55.16947.

Rick, J.W., 1987. Dates as data: an examination of the Peruvian preceramic radiocarbon record. Am. Antiq. 52, 55. https://doi.org/10.2307/281060.
Riris, P., 2018. Dates as data revisited: a statistical examination of the Peruvian preceramic radiocarbon record. J. Archaeol. Sci. 97, 67–76. https://doi.org/10.1016/j.jas.2018.06.008.
Roberts Jr., J.M., Mills, B.J., Clark, J.J., Haas Jr., W.R., Huntley, D.L., Trowbridge, M.A., 2012. A method for chronological apportioning of ceramic assemblages. J. Archaeol. Sci. 39, 1513–1520. https://doi.org/10.1016/j.jas.2011.12.022.
Rogers, E.M., 1962. Diffusion of Innovations, first ed. Free Press of Glencoe, New York.
Sekine, T., 2014. Aomori-ken ni okeru Jōmon jidai no iseki-su no hensen. Quat. Res. (Daiyonki kenkyu) 2014 (53), 193–203 (In Japanese).
Shishikura, M., Echigo, T., Kaneda, H., 2007. Marine reservoir correction for the Pacific coast of central Japan using 14C ages of marine mollusks uplifted during historical earthquakes. Quat. Res. 67, 286–291. https://doi.org/10.1016/j.yqres.2006.09.003.
Shitara, H., 2004. Saiso no haikei - Jōmon/Yayoi jidai ni okeru kankyō hendō tono taiōkankei. Kokuritsu rekishi minzoku hakubutsukan kenkyū hōkoku 112, 357–380 (In Japanese).
Shennan, S., Downey, S.S., Timpson, A., Edinborough, K., Colledge, S., Kerig, T., Manning, K., Thomas, M.G., 2013. Regional population collapse followed initial agriculture booms in mid-Holocene Europe. Nat. Commun. 4 https://doi.org/10.1038/ncomms3486 ncomms3486.
Steponaitis, V.P., Kintigh, K.W., 1993. Estimating site occupation spans from dated artifact types: some new approaches. In: Stoltman, J. (Ed.), Archaeology of Eastern North America: Papers in Honor of Stephen Williams. Archaeological Report No. 25. Mississippi Department of Archives and History, Jackson, pp. 349–361.
Surovell, T.A., Toohey, J.L., Myers, A.D., LaBelle, J.M., Ahern, J.C.M., Reisig, B., 2017. The end of archaeological discovery. Am. Antiq. 1–13. https://doi.org/10.1017/aaq.2016.33.
Suzuki, Y., 2006. Jōmonjidai Shūraku No Kenkyū. Yūzankaku, Tokyo (In Japanese).
Suzuki, Y., 2009. Kantō/Tōkai chihō no Jōmon shūraku to Jōmon shakai. In: Suzuki, K., Suzuki, Y. (Eds.), Shūraku No Hensen to Chiikisei. Tokyo, Yūzankaku, pp. 95–143 (In Japanese).
Tallavaara, M., Pesonen, P., 2018. Human ecodynamics in the north-west coast of Finland 10,000–2000 years ago. Quat. Int. https://doi.org/10.1016/j.quaint.2018.06.032.
Taniguchi, Y., 2005. Kanjōshūraku to Jōmon Shakaikōzō. Gakuseisha, Tokyo (In Japanese).
Taniguchi, Y., 2019. Nyūmon Jōmonjidai No Kōkogaku. Dōseisha, Tokyo (In Japanese).
Timpson, A., Colledge, S., Crema, E., Edinborough, K., Kerig, T., Manning, K., Thomas, M.G., Shennan, S., 2014. Reconstructing regional population fluctuations in the European Neolithic using radiocarbon dates: a new case-study using an improved method. J. Archaeol. Sci. 52, 549–557. https://doi.org/10.1016/j.jas.2014.08.011.
Toda, T., 1999. Kantō-chihō chūki (Kasori E shiki). Jōmonjidai 10, 298–307 (In Japanese).
Torfing, T., 2015. Neolithic population and summed probability distribution of 14C-dates. J. Archaeol. Sci. 63, 193–198. https://doi.org/10.1016/j.jas.2015.06.004.
Tsuji, S., 2013. Jōmonjidai no nendai to rikuiki no seitaikeishi. In: Izumi, T., Imamura, K. (Eds.), Kōza Nihon No Kōkogaku 3: Jōmon-Jidai 1, pp. 61–81 (In Japanese).
Watanabe, H., 1986. Community habitation and food gathering in prehistoric Japan: an ethnographic interpretation of the archaeological evidence. In: Pearson, R.J., Barnes, G.L., Hutterer, K.L. (Eds.), Windows on the Japanese Past: Studies in Archaeology and Prehistory. Centre for Japanese Studies University of Michigan, Ann Arbor, pp. 229–254.
Williams, A.N., 2012. The use of summed radiocarbon probability distributions in archaeology: a review of methods. J. Archaeol. Sci. 39, 578–589.
Weninger, B., Clare, L., Jöris, O., Jung, R., Edinborough, K., 2015. Quantum theory of radiocarbon calibration. World Archaeol. 47, 543–566. https://doi.org/10.1080/00438243.2015.1064022.
Yasuda, Y., 2004. Sekaishi No Naka No Jōmon Bunka, third ed. Yūzankaku, Tokyo (In Japanese).
Zahid, H.J., Robinson, E., Kelly, R.L., 2016. Agriculture, population growth, and statistical analysis of the radiocarbon record. Proc. Natl. Acad. Sci. Unit. States Am. 113, 931–935. https://doi.org/10.1073/pnas.1517650112.
Ziedler, J.A., Buck, C.E., Litton, C.D., 1998. Integration of archaeological phase information and radiocarbon results from the jama river valley, Ecuador: a bayesian approach. Lat. Am. Antiq. 9, 160–179.